

Predicting nucleation near the spinodal in the Ising model using machine learning

Shan Huang*

*Department of Physics, Boston University,
Boston, Massachusetts 02215, USA*

William Klein†

*Department of Physics, Boston University,
Boston, Massachusetts 02215, USA and
Center for Computational Science, Boston University,
Boston, Massachusetts 02215, USA*

Harvey Gould

*Department of Physics, Boston University,
Boston, Massachusetts 02215, USA and
Department of Physics, Clark University,
Worcester, Massachusetts 01610, USA*

Abstract

We use the Convolutional Neural Network (CNN) and two logistic regression models to predict the occurrence of nucleation in the nearest-neighbor and long two-dimensional Ising model. The CNN outperforms the latter models for both interaction ranges and all system sizes, especially as the size of the system becomes large. We find that the the ability of all three methods to predict the nucleation probability decreases as system becomes closer to the spinodal for the long-range Ising model. We explain this decrease as due to the ramified droplet structure of the nucleating droplet near the spinodal.

* sh2015@bu.edu

† klein@bu.edu

I. INTRODUCTION

Nucleation plays an important role in various natural phenomena, including, for example, the formation of rain drops [1], the liquid-solid phase transition, and dynamic damage in multiphase materials [2]. In many technological applications, such as artificial precipitation [3], growth of semiconductor thin films [4], synthesis of protein [5], it is important to be able to predict, trigger, or prevent nucleation.

Classical nucleation theory [6] assumes that there is a clear boundary between the nucleating droplet and the background and the compact nucleating droplet. However, this assumption breaks down when the system is quenched deeper into the metastable regime, near a spinodal [7–9]. Spinodal nucleation has been observed in various simulations, such as the long-range Ising model [10] and Lenard-Jones dense liquids [11], producing nucleating droplet with a compact core and ramified halo [12, 13]. The system has a flat free energy landscape, making it difficult to determine the existence of critical droplets.

In the last decade machine learning has demonstrated astonishing power in various prediction problems. For example, Hu [14] et al. applied Principal Component Analysis, an unsupervised learning clustering technique, to classify the disordered and ordered states and find phase transition in the Ising and Blume-Capel models. Carrasquilla [15] et al. used neural networks to made similar predictions for disordered or topological systems with no classical order parameters. Pun [16] et al. used a Convolutional Neural Network (CNN) [17] to make predictions of the event sizes in the Olami-Feder-Christensen model.

In this paper we apply several machine learning methods to predict the occurrence of nucleation in the both the nearest-neighbor and long-range Ising models. In Sec. II we discuss the intervention method that we use to obtain data to train the machine learning models. In Sec. III we introduce the machine learning models that we use to do the prediction task, including two Logistic Regression models and a CNN model. In Sec. IV we compare the performance of these models and show that the CNN is more successful and robust for larger systems. We observe a decrease in predictability near the spinodal in the long-range Ising model. In Sec. V we use occlusion analysis to identify the region of importance identified by xx and find the region overlaps with the largest cluster found by a percolation mapping. The region of importance increase in size and decrease in sensitivity as the system is quenched closer to the closer to spinodal. We explain the decrease of predictability as using spinodal

nucleation theory.

II. DATA ACQUISITION

Our simulations are performed using the Metropolis algorithm. The system is first equilibrated at temperature $T = 4/9T_c$ with the magnetic field h pointing up. We consider both the nearest-neighbor Ising model with $T_x = xx$ and the long-range Ising model with interaction range $R = 10$ for which we take $T_c = 4$. We then flip the magnetic field to the down direction so that the system is in a metastable state. The average lifetime of metastable state in our simulations is around 10^4 . Due to thermal fluctuation, clusters consisting of spins pointing in the down direction will grow and vanish. Eventually, a cluster will overcome the free energy barrier and grow until it occupies the whole system. The time it takes for the nucleating droplet to grow to at least half the size of the system is approximately 50 Monte Carlo steps per spin (MCS) for $R = 1$ and 20 MCS for $R = 10$ for systems with linear dimension $L = 10R$. The simulation is terminated when the magnetization m becomes negative.

Our goal can be expressed as follows: given a 2D Ising configuration X as input, we wish to train a statistical model to predict the nucleation probability p_{nuc} . p_{nuc} denotes the probability that nucleation will occur within a short period of time t_{nuc} in Ising configuration X . Here we identify the occurrence of nucleation as magnetization m becomes negative. We obtain p_{nuc} through intervention method, and minimize discrepancy between predicted value \hat{p}_{nuc} and true value p_{nuc} .

We attempt to predict \hat{p}_{nuc} on Ising models with different interaction range varying from $R = 1$ to $R \sim 10$. We take the linear dimension of the system L to be at least ten times greater than R to avoid finite size effects. The total number of spins is $N = L^2$.

A. Intervention method

We measure time t in MCS and take $t = 0$ to be the time that m first becomes negative and the simulation is stopped. We keep a record of the spin configurations of every MCS for the the last 50 MCS. The intervention method proceeds by making n_{int} copies of the system at a given intervention time $t_{\text{int}} < 0$ and then running each copy with a different random

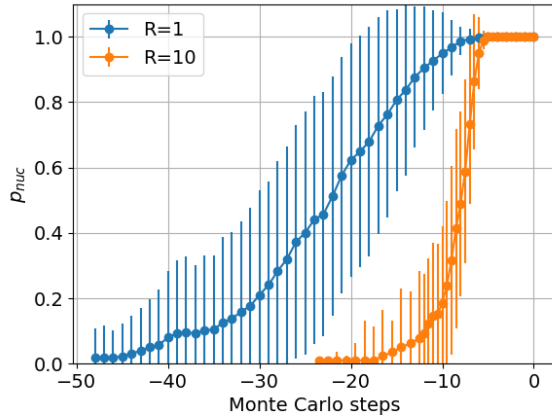


FIG. 1: The evolution of the nucleation probability p_{nuc} . At $t = 0$, more than half of the spins have flipped to the stable direction, and nucleation has already occurred before this time. Results are shown for $R = 1$, $L = 10$, $\Delta h = 0.70$ and $R = 10$, $L = 100$, $\Delta h = 0.055$.

number seed, and determine the number of copies that reach $m < 0$ at roughly $t = 0$ (we allow a difference within 10 MCS). We denote this time window with $t_{\text{nuc}} = 0 - t_{\text{int}}$. The nucleation probability at time t is given by $p_{\text{nuc}} = n_{\text{nuc}}/n_{\text{int}}$. We choose $n_{\text{int}} = 100$. A typical result for p_{nuc} from the intervention method is given in Fig. 1.

We did not monitor if the copies nucleated at the same position as the original run. Considering that the size of our system is relatively small and the time window that we monitor is short, it is very unlikely to happen that another nucleus could form and complete the nucleation process, while the original nucleus dies during the time we are monitoring the system, because t_{nuc} is relatively small.

B. Dataset preparation

Due to the nature of the intervention method, there are a lot of data points where $p_{\text{nuc}} \approx 0$ or $p_{\text{nuc}} \approx 1$ in our original dataset, but much fewer in the middle. To ensure predictions from trained model does not favor these two values, we discard data points according to how often their corresponding p_{nuc} occur, so that in our final dataset, we have a uniform distribution of p_{nuc} .

To ensure a uniform distribution

Because machine learning methods we use do not take periodic boundary conditions into

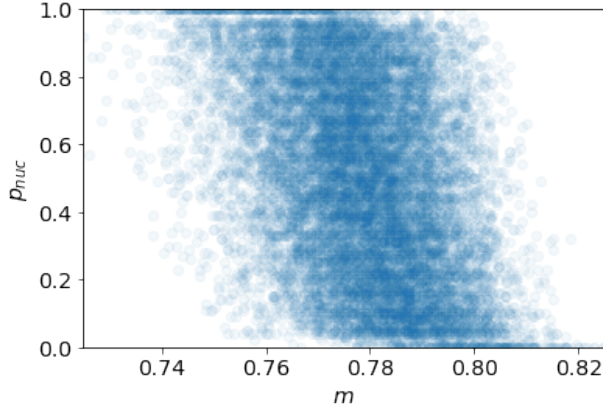


FIG. 2: The measured nucleation probability p_{nuc} versus the magnetization m for $R = 10$ and $\Delta h = 0.055$. Note that the value of m is not sufficient for predicting p_{nuc} .

account, we translate each spin configuration so that the center of mass of the largest cluster is in the center of the simulation box. The clusters are determined using the Coniglio-Klein percolation mapping [18].

We divide the dataset into training and testing datasets. The former is used to train the machine learning model and the latter is for testing model performance by comparing model's prediction \hat{p}_{nuc} and the p_{nuc} obtained from intervention.

Before we apply machine learning models, we have to ensure that there is no obvious relation between the nucleation probability and the magnetization m . Figure 2 shows that there is only a very weak correlation between p_{nuc} and m .

III. MACHINE LEARNING MODELS

We applied three models: spin-based logistic regression, features-based logistic regression, and Convolutional Neural Network (CNN).

A. Spin-based logistic regression

For the spin-based logistic regression methods, the spin configuration is represented by a one-dimensional N -element array, with each element corresponding to a spin. A logistic regression model is trained and tested on this representation as the baseline. This method

takes into account the location and density of the spins in the stable direction, but, by its nature, does not consider local spatial correlations.

B. Features-based logistic regression

To take the spatial correlation of the configurations into account, we introduce features-based logistic regression. The idea is to construct a higher level representation of the configuration with some hand-crafted geometric quantities, and use this representation as the input to the logistic regression model. This way, the input becomes more concise and efficient, but less complete. It is able to tell us which of the features are important, but incapable of discovering new features.

C. Convolutional Neural Network

Convolutional Neural Network has several advantages in carrying out our task: First, it uses convolution operations to help look for local geometric correlations. Second, the convolution filters sweep through each site in the input, granting it translation invariance. Third, CNN uses raw configuration as input, so it has access to complete information.

We use two CNN model structures in our study, one simpler, the other more complicated. The simpler one consists of 2 layers, number of filters in the layers are 8 and 16, which we use in comparing the performance of CNN to the other two models mentioned above, in most generic cases ($1 \leq R \leq 10$, $10 \leq L \leq 100$). The more complicated one consists of 4 layers, number of filters in each layer is 8, 16, 32, 64, which we used in studying predictability when system gets closer to spinodal ($R = 12, 15, 18, 20$; $L = 200$). Because in this case, we need enough model complexity to exhaust the predictability. There is a maxpool layer between every two convolution layers, with pooling size of 2 and stride of 1, followed by a ReLU nonlinear layer. The output is then passed into a linear layer with 100 neurons, followed by another ReLU activation. A final linear layer is placed with softmax activation that transforms the result into a two element vector, representing $(\hat{p}_{\text{nuc}}, 1 - \hat{p}_{\text{nuc}})$. We also applied a dropout layer in between CNN layers with a dropout rate of 0.15 [19].

The models are trained with ADAM optimizer [20] minimizing cross entropy loss. An early stopping with patience of 10 epochs is performed to prevent overfitting.

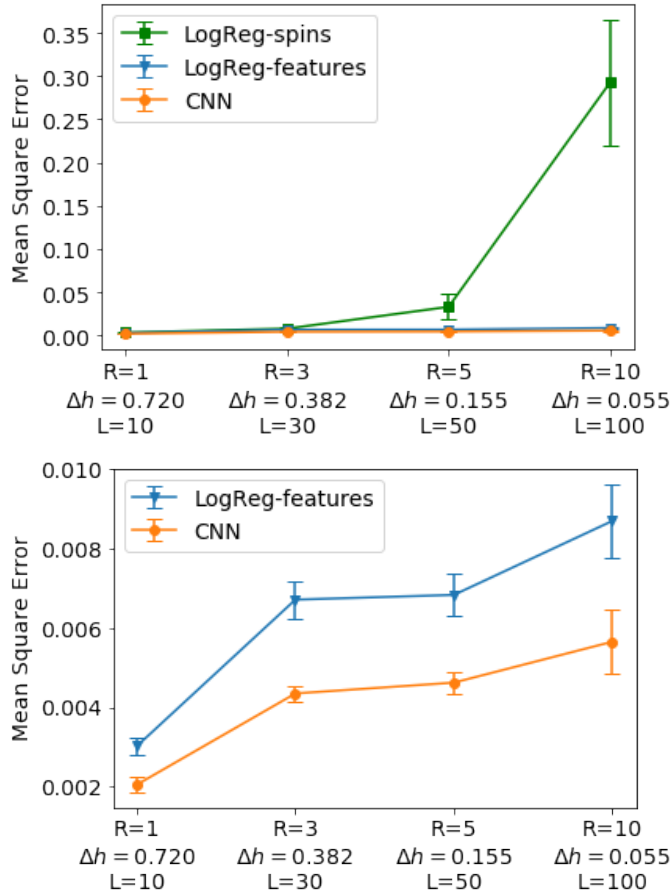


FIG. 3: Comparison of the performance of simple logistic regression, feature based logistic regression, and CNN. We used a two Layer CNN with filter numbers 8 and 16. The mean square error was averaged over a 10-fold cross validation. (a) CNN is applicable over a wide range of R and L in contrast to spin-based logistic regression. (b) CNN outperforms features-based logistic regression.

IV. RESULTS

A. Performance on generic systems

In this section, we present the performance of the three methods in Ising systems with different size and interaction range varying from classical nucleation to near spinodal nucle-

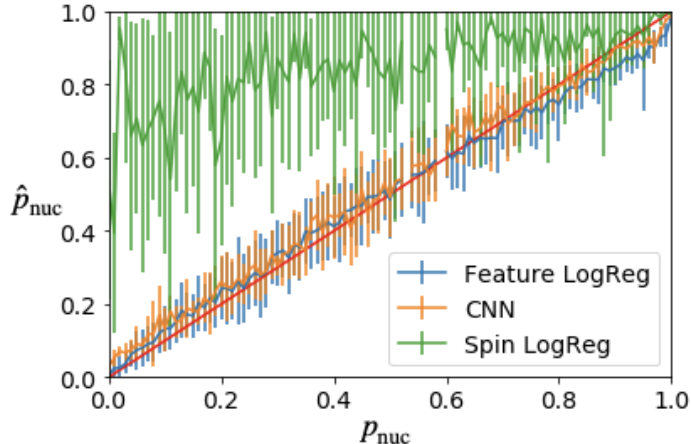


FIG. 4: Confusion plot of three models for $R = 10$, $L = 100$, $\Delta h = 0.055$. The red line is perfect prediction. CNN performs slightly better than features-based logistic regression, while both models perform much better than spin-based logistic regression.

ation, with $R = 1, 3, 5, 10$ with $L = 10R$. We vary the magnetic field in each system (shown in Fig. 3) so that the Ginsburg Parameter is the same in all of our simulations. One model is trained for each method in each system. The models were trained on 12000 data points (each data point refers to a spin configuration and a value of p_{nuc}) and tested on 2000 data points. We use a 10-fold cross-validation [21].

As is shown in Fig. 3, the accuracy of the predictions of spin-based logistic regression decreases, even vanishes completely as R and L become larger. The main reason is that logistic regression models have very few learnable parameters. For $R = 1$, $L = 10$, the input size is a $N = L^2 = 100$ dimensional vector, whereas for $R = 10$, the input size is $N = 10^4$. The model complexity of logistic regression is not sufficient for such large inputs.

Features-based logistic regression overcomes the problem of exceedingly large inputs. By hand-crafting features from the raw configuration, we reduce the dimension of the input to a fixed number $n_{\text{features}} \sim 10$. The features that we choose are the magnetization m , the average distance to the center of mass of largest cluster $R^{(1)}$ and its higher moments $R^{(k)}$. Namely, our input vector is

$$X = (m, R^{(1)}, R^{(2)} \dots R^{(n)}) \quad (1)$$

$$R^{(k)} = \left(\frac{1}{N_s} \sum_i^{N_s} r_i^k \right)^{1/k}, \quad (2)$$

where N_s is the number of spins in the stable direction, r_i is the distance of spin i to the

center of mass of the largest cluster. This quantity is summed over all spins that point in the stable direction. In our model, we calculate up to the 9th moment of distance. This simple model works well in all systems, achieving an average absolute error of less than 0.1 even for systems with $R = 10$, $L = 100$.

As shown in Figs. 3 and 4, CNN outperforms the two logistic regression models for values of R and L . It achieves a mean-square error as small as 5.65×10^{-3} for the largest R considered (equivalent to an average error of 0.075). In terms of the mean square error CNN outperforms features-based logistic regression by around 40% for all values of R . The ability to make predictions decreases only slightly as the input size becomes bigger. This is because the learnable parameters of CNN are weights in convolution filters, whose complexity does not scale as the input gets larger.

B. Predictability of near-spinodal systems

In Ref. [16], it was found that the closer the OFC model is to a critical point, the less predictable the system. Their goal was to predict the event size within one plate update given the stress configuration of the system. They found that at the noise-induced critical point, the system loses predictability completely. In this section, we test if a similar effect occurs in the Ising model near the spinodal, an example of a mean-field critical point. We expect to find a significant decrease of the predictability as the spinodal is approached.

The spinodal magnetic field in the long-range Ising model is $h_s \approx 1.27$. To ensure that the lifetime of the metastable state is at least 10^4 MCS, we increased the interaction range R at the same time as we increased h toward h_s . However, we keep $L = 200$, to ensure that input size is not a factor when we compare performance of same CNN model structure. Each model was trained on 7000 data points and validated on 1000 data points.

Our results are shown in Fig. 5. Each data point represents the mean square error of the model when making predictions for the corresponding Ising system, the error bar is calculated based on a 10-fold cross-validation. As h approaches h_s , the model exhibits worse performance. The mean square error increases from 0.0052 to 0.0174 (equivalent to increase of average discrepancy between \hat{p}_{nuc} and p_{nuc} from 0.072 to 0.132).

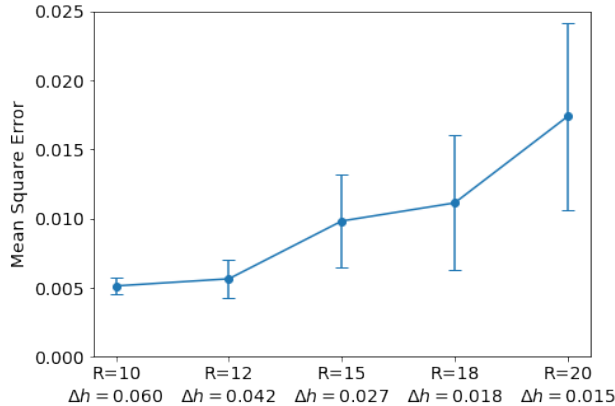


FIG. 5: Comparison of the performance of the same CNN model (with 4 layers, number of filters in layers to be 8, 16, 32, 64) with same input size as the the magnetic field approaches h_s . As the system gets closer to spinodal, CNN model demonstrates a worse and more unstable performance.

V. DISCUSSION

We used CNN and feature based logistic regression to make reasonable predictions of p_{nuc} . To help us to gain a deeper insight into the mechanism of nucleation, we now study the models themselves, looking at their learnable parameters and their behavior to understand how the models make predictions.

A. Important geometric quantities: m and $R^{(1)}$

Logistic regression models can be summarized in Eq. 3:

$$\hat{p}_{\text{nuc}}(X) = \frac{1}{1 + \exp(-\sum_{i=1}^{n_{\text{features}}} \beta_i X_i)} \quad (3)$$

where β is the weight vector, that has same size as the input vector. Each of its component β_i corresponds to a feature X_i . The bigger β_i is, the more important feature X_i is. Therefore, Logistic regression can be interpreted by investigating the weight vector.

Fig. 6 shows the weight vector in features-based logistic regression in both the nearest neighbor and long range ($R = 10$) Ising models. It shows that in both cases the most important features are the magnetization m (positively correlated) and the first moment of $R^{(1)}$ (negatively correlated). These correlations are expected: the bigger number of spins that are in the stable direction, the more likely nucleation will occur. And the less dense the

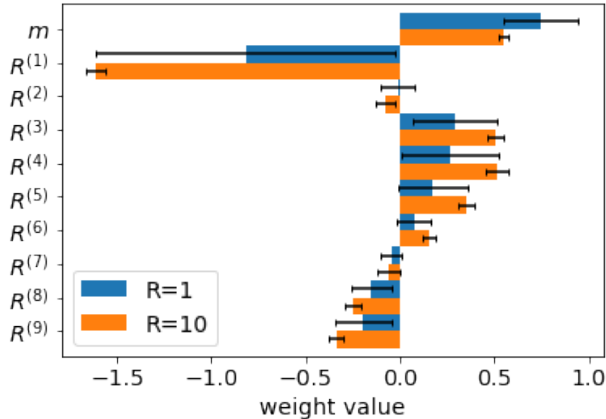


FIG. 6: Weights corresponding to each geometric features in features-based logistic regression (averaged using cross-validation). The most important features are the magnetization m and the first moment $R^{(1)}$.

spins are in the vicinity of the largest cluster, the less likely nucleation is going to happen. Also note that the higher moments $R^{(i)}$ is much more important in long range systems than in nearest neighbor systems, which means that in long range systems, the outer spins plays more important roles than the inner spins (since outer spins amplifies higher order $R^{(i)}$ more than lower order $R^{(i)}$). This agrees with the prediction by spinodal nucleation theory that in long-range systems, the critical cluster have a much larger spatial span.

B. Region of importance: Critical cluster

Occlusion analysis [22] is commonly used to visualize and understand what the Convolutional Neural Network has learned. This analysis is done by randomly choosing a small region in the two-dimensional input and replacing the values in that region by zeros, called occluded input, and observing how much the predictions of the model vary when fed the original and occluded inputs. The bigger the difference, the more important the replaced region. This process is repeated many times to obtain an occlusion sensitivity map [22], which illustrates how important each part of the input is.

We implemented the occlusion analysis by replacing the spins in the chosen region by zeros (instead of ± 1 in the original input). An example of an occlusion result is shown in Fig. 7 for $R = 10$, $h = 1.21$, averaged over the test set. As expected, the most important region is the center, because our input is already centered around the largest cluster in the

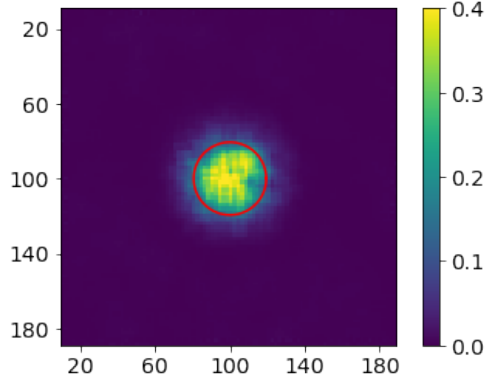


FIG. 7: Occlusion map for $R = 10$, $\Delta h = 0.06$, $L = 200$. The red circle is the radius of gyration of the biggest cluster, which overlaps with the high impact region of the occlusion map. This result shows that biggest cluster is important in determining the likelihood of nucleation.

system. What is worth noting is the size of the important region. We calculated the average radius of gyration of the largest cluster over the entire test set for $R = 10$, $\overline{R}_g = 19.42$. As shown in Fig. 7, the radius of the important region is comparable to the calculated \overline{R}_g , shown by the red circle. This consistency indicates that the machine acquires useful geometric information for predictions from the region occupied by the largest cluster.

C. Dilution of important region and lost of predictability at spinodal

Occlusion analyses were done on systems closer to spinodal where $h \rightarrow h_s$, $10 < R \leq 20$, $L = 200$, shown in Fig. 8. As we get closer to spinodal, we observe that the region of importance expands spatially while the overall sensitivity decreases. The size of the important region is always comparable with the region occupied by the largest cluster in the system, shown in red circle.

In the field theory developed by W. Klein et al. [9], they predicted that droplet in long range interaction (but not mean field) systems has a dense core and a ramified hallow. As the spinodal is approached, the core shrinks and the droplet becomes more and more ramified, shown in Fig. 9 (a) [23]. When spinodal is reached, the core would disappear and the droplet has a density equal to the background. The blue curves in Fig. 9 (b) shows that droplet density behaves similar to that in our simulation. More over, it shows that occlusion

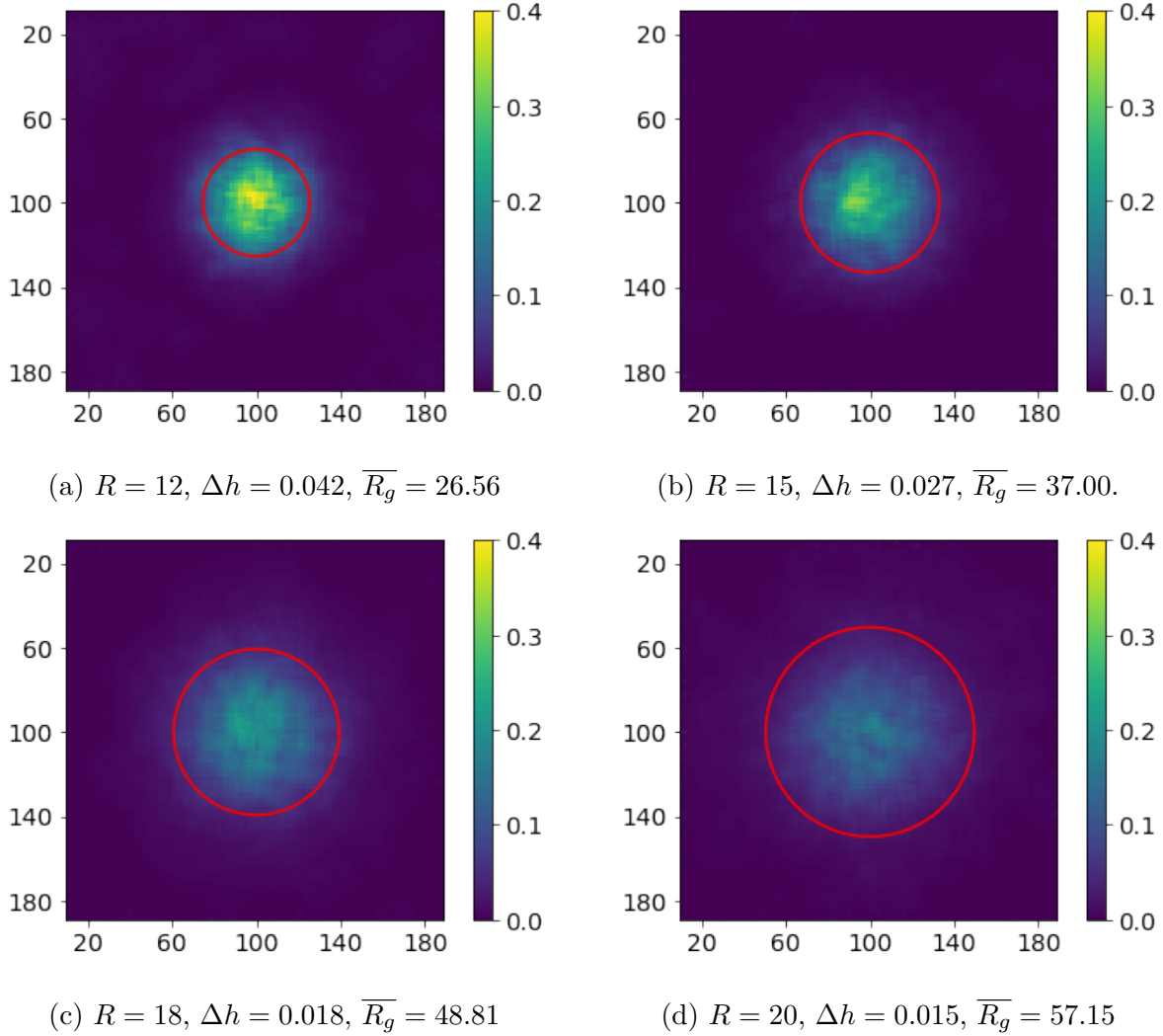


FIG. 8: Occlusion maps for systems closer to spinodal. Region circled by red line stands for region occupied by critical clusters. As the system gets closer to spinodal, the region of importance becomes larger but weaker. Its size scales as size of critical cluster and its intensity is more diluted similar to the density of critical droplet.

sensitivity (red curves) is strongly correlated to droplet density.

Based on the above theory and what we observed from Fig. 8 and Fig. 9 (b), we give explanation to the decrease of predictability as follows: The CNN model acquires information for prediction mainly from higher density regions, which correspond to region occupied by the largest droplet. As system get closer to spinodal, the droplet ramifies, its density decreases, and becomes more and more similar to the background. It follows that the systems with larger nucleating droplets (which have higher p_{nuc}) becomes indistinguishable from systems

with smaller nucleating droplets. As a result, the CNN model performs worse and worse.

VI. CONCLUSION

In this paper we proposed methods of using machine learning in predicting classical and spinodal nucleation in Ising model. Among them, CNN performs well in all different systems tested. We observed a decrease in predictability as system gets closer to spinodal, and gave explanation with the help of occlusion analyses.

features-based logistic regression attempts to do a dimension reduction task, representing complex Ising configurations with a few hand-crafted geometric quantities that carries limited but essential information. It has an acceptable performance even in large and long interaction range systems. It is also shown to be useful in identifying important geometric features that determines the dynamics of spinodal nucleation.

Convolutional Neural Network outperforms other methods we attempted and is able to make closely accurate predictions. The performance stays pretty good and stable even when large inputs are given. Using occlusion method as analyses tool for CNN, we discovered that CNN obtains its information mainly from region occupied by the largest droplet, especially the dense core part. The predictability vanishes as the Ising system gets very close to spinodal (which is a critical point), due to the vanishing difference between nucleating droplet and the background. This result echoes with Pun's observation in near-critical OFC model [16].

The method of using CNN to predict nucleation can be easily generalized to systems other than Ising model, especially ones that are hard to make accurate predictions with statistical mechanics theories. Examples are: crystallization in Lenard-Jones dense liquid, breakdown of a neural system, evolution of cellular automaton. The next steps of our study will be implementing CNN and other machine learning models on Lenard Jones liquid-solid phase transition, which also demonstrates characteristics of spinodal nucleation, and check

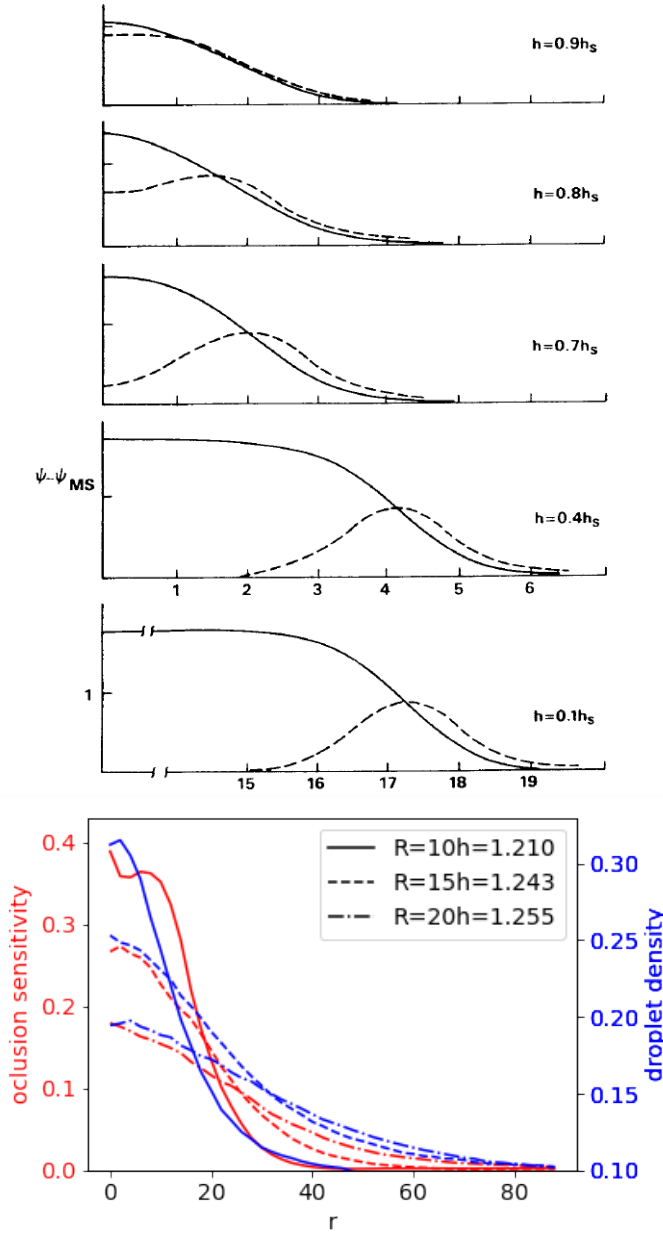


FIG. 9: (a)Change of droplet density profile when $h \rightarrow h_s = 1.27$. The droplet core shrinks while hallow expands, resulting a more and more ramified droplet. (b)Comparison between occlusion sensitivity and droplet density, r is the distance away from center of mass of largest droplet in the system. Red lines represents occlusion sensitivity and blue lines represents droplet density. It is shown that two quantities strongly correlate with each other. As $h \rightarrow h_s$, the droplet expands and ramifies, accompanied by expansion of important region and decrease of sensitivity

if approaching the critical point there also results in a vanishing predictability.

- [1] U. Dusek, G. Frank, L. Hildebrandt, J. Curtius, J. Schneider, S. Walter, D. Chand, F. Drewnick, S. Hings, D. Jung, *et al.*, Size matters more than chemistry for cloud-nucleating ability of aerosol particles, *Science* **312**, 1375 (2006).
- [2] S. Fensin, J. Escobedo, G. Gray III, B. Patterson, C. Trujillo, and E. Cerreta, Dynamic damage nucleation and evolution in multiphase materials, *Journal of Applied Physics* **115**, 203516 (2014).
- [3] R. R. Braham, L. J. Battan, and H. R. Byers, Artificial nucleation of cumulus clouds, in *Cloud and Weather Modification* (Springer, 1957) pp. 47–85.
- [4] R. Ueda, Nucleation, growth processes, and electrical properties of semiconductor thin films, in *Rost Kristallov/Growth of Crystals* (Springer, 1979) pp. 64–66.
- [5] R. P. Sear, Nucleation: theory and applications to protein solutions and colloidal suspensions, *Journal of Physics: Condensed Matter* **19**, 033101 (2007).
- [6] R. Becker and W. Döring, Kinetische behandlung der keimbildung in übersättigten dämpfen, *Annalen der Physik* **416**, 719 (1935).
- [7] W. Klein and C. Unger, Pseudospinodals, spinodals, and nucleation, *Physical Review B* **28**, 445 (1983).
- [8] C. Unger and W. Klein, Nucleation theory near the classical spinodal, *Physical Review B* **29**, 2698 (1984).
- [9] C. Unger and W. Klein, Initial-growth modes of nucleation droplets, *Physical Review B* **31**, 6127 (1985).
- [10] L. Monette, Spinodal nucleation, *International Journal of Modern Physics B* **8**, 1417 (1994).
- [11] R. Verma, *A supercooled study of nucleation and symmetries*, Ph.D. thesis, Boston University (2018).
- [12] D. W. Heermann and W. Klein, Nucleation and growth of nonclassical droplets, *Physical review letters* **50**, 1062 (1983).
- [13] K. Barros and W. Klein, Liquid to solid nucleation via onion structure droplets, *The Journal of chemical physics* **139**, 174505 (2013).
- [14] W. Hu, R. R. Singh, and R. T. Scalettar, Discovering phases, phase transitions, and crossovers

- through unsupervised machine learning: A critical examination, *Physical Review E* **95**, 062122 (2017).
- [15] J. Carrasquilla and R. G. Melko, Machine learning phases of matter, *Nature Physics* **13**, 431 (2017).
- [16] C.-K. Pun, S. Matin, W. Klein, and H. Gould, Prediction in a driven-dissipative system displaying a continuous phase transition, arXiv preprint arXiv:1907.11790 (2019).
- [17] A. Krizhevsky, I. Sutskever, and G. E. Hinton, Imagenet classification with deep convolutional neural networks, in *Advances in neural information processing systems* (2012) pp. 1097–1105.
- [18] A. Coniglio and W. Klein, Clusters and ising critical droplets: a renormalisation group approach, *Journal of Physics A: Mathematical and General* **13**, 2775 (1980).
- [19] N. Srivastava, G. Hinton, A. Krizhevsky, I. Sutskever, and R. Salakhutdinov, Dropout: a simple way to prevent neural networks from overfitting, *The journal of machine learning research* **15**, 1929 (2014).
- [20] D. P. Kingma and J. Ba, Adam: A method for stochastic optimization, arXiv preprint arXiv:1412.6980 (2014).
- [21] R. Kohavi *et al.*, A study of cross-validation and bootstrap for accuracy estimation and model selection, in *Ijcai*, Vol. 14 (Montreal, Canada, 1995) pp. 1137–1145.
- [22] M. D. Zeiler and R. Fergus, Visualizing and understanding convolutional networks, in *European conference on computer vision* (Springer, 2014) pp. 818–833.
- [23] K. Binder, The monte carlo method for the study of phase transitions: A review of some recent progress, *Journal of Computational Physics* **59**, 1 (1985).